frontiers in Astronomy and Space Sciences

METHODS
published: 28 February 2019
doi: 10.3389/fspas.2019.00008

JWST/NIRSpec Prospects on Transneptunian Objects

Robin Métayer[1], Aurélie Guilbert-Lepoutre[1,2], Pierre Ferruit[3], Frédéric Merlin[4], Bryan J. Holler[5], Nahuel Cabral[2] and Cathy Quantin-Nataf[1]*

[1] LGLTPE, UMR 5276 CNRS, Université de Lyon, Université Claude Bernard Lyon 1, ENS Lyon, Villeurbanne, France, [2] UTINAM, UMR 6213 CNRS, UBFC, Besançon, France, [3] ESA, ESTEC, Noordwijk, Netherlands, [4] LESIA-Observatoire de Paris, UMR 8109 CNRS, UPMC Univ Paris 06, Univ. Denis Diderot, Sorbonne Paris Cite, Meudon, France, [5] STScI, Baltimore, MD, United States

The transneptunian region has proven to be a valuable probe to test models of the formation and evolution of the solar system. To further advance our current knowledge of these early stages requires an increased knowledge of the physical properties of Transneptunian Objects (TNOs). Colors and albedos have been the best way so far to classify and study the surface properties of a large number TNOs. However, they only provide a limited fraction of the compositional information, required for understanding the physical and chemical processes to which these objects have been exposed since their formation. This can be better achieved by near-infrared (NIR) spectroscopy, since water ice, hydrocarbons, and nitrile compounds display diagnostic absorption bands in this wavelength range. Visible and NIR spectra taken from ground-based facilities have been observed for ∼80 objects so far, covering the full range of spectral types: from neutral to extremely red with respect to the Sun, featureless to volatile-bearing and volatile-dominated (Barkume et al., 2008; Guilbert et al., 2009; Barucci et al., 2011; Brown, 2012). The largest TNOs are bright and thus allow for detailed and reliable spectroscopy: they exhibit complex surface compositions, including water ice, methane, ammonia, and nitrogen. Smaller objects are more difficult to observe even from the largest telescopes in the world. In order to further constrain the inventory of volatiles and organics in the solar system, and understand the physical and chemical evolution of these bodies, high-quality NIR spectra of a larger sample of TNOs need to be observed. JWST/NIRSpec is expected to provide a substantial improvement in this regard, by increasing both the quality of observed spectra and the number of observed objects. In this paper, we review the current knowledge of TNO properties and provide diagnostics for using NIRSpec to constrain TNO surface compositions.

Keywords: method: observational, technique: spectroscopic, telescope: JWST, kuiper belt: general, minor planets and asteroids: general

OPEN ACCESS

Edited by:
Patryk Sofia Lykawka, Kindai University, Japan

Reviewed by:
Bojan Novakovic, University of Belgrade, Serbia
Susan D. Benecchi, Planetary Science Institute, United States

***Correspondence:**
Aurélie Guilbert-Lepoutre
aurelie.guilbert-lepoutre@univ-lyon1.fr

Specialty section:
This article was submitted to Fundamental Astronomy, a section of the journal Frontiers in Astronomy and Space Sciences

Received: *10 September 2018*
Accepted: *30 January 2019*
Published: *28 February 2019*

Citation:
Métayer R, Guilbert-Lepoutre A, Ferruit P, Merlin F, Holler BJ, Cabral N and Quantin-Nataf C (2019) JWST/NIRSpec Prospects on Transneptunian Objects. Front. Astron. Space Sci. 6:8. doi: 10.3389/fspas.2019.00008

INTRODUCTION

The outer solar system is occupied by a vast population of icy objects orbiting beyond Neptune, generally referred to as Transneptunian Objects (TNOs). They hold valuable information on the chemical and physical conditions that prevailed in the early solar system, in this critical region of the protoplanetary disk where various ice lines were located (for example, the H_2O ice line may have been located from 2 to 5 au, and the CO snowline from 8 to 12 au during the evolution of the

Sun's protoplanetary disk, (Dodson-Robinson et al., 2009). Since the discovery of the first object labeled as such in 1992 (Jewitt and Luu, 1993), it has become very clear that these bodies can be divided into sub-populations—broadly speaking five categories—based on their orbital properties (Gladman et al., 2008):

- The Classical Belt, also known as the Kuiper Belt, made of two dynamical components—the Cold Classical Objects and Hot Classical Objects (Nesvorny, 2015b). Overall, they form a donut-shaped structure roughly located between the 3:2 and 2:1 mean-motion resonances with Neptune. Cold objects have relatively unperturbed orbits, with low inclination and very small eccentricity.
- Resonant objects, including Pluto, with orbits in mean-motion resonance with Neptune.
- Scattered Disk objects, with perihelion distances larger than 30 au, and sometimes extreme orbits with large eccentricities (up to 0.8) and high inclinations. The orbits of scattered disk objects are unstable on the timescale of the age of the solar system.
- Detached objects, with perihelion distances sufficiently large to avoid the gravitational influence of Neptune or other planets.
- Centaurs form an additional class of objects. They are TNOs, coming either from the scattered disk or the hot classical population, which got destabilized toward an unstable orbit in the giant planet region.

The existence and characteristics of these sub-populations (see Lacerda et al., 2014 or Jewitt, 2015 for instance) implies that this remnant of the Sun's protoplanetary disk was shaped by complex dynamical processes. In particular, it suggests that the giant planets underwent a phase of migration and dynamical instability, such as described for example in the Nice model (Gomes et al., 2005; Morbidelli et al., 2005; Tsiganis et al., 2005). As of today, not one model can reproduce the complex architecture observed in the transneptunian region. However, studies of the giant planets' migration (gas- or planetesimal-driven) at different stages of the solar system, and for instance the detailed investigation of Neptune's migration (Nesvorny and Vokrouhlicky, 2016), have brought us a clearer picture of how the solar system evolved since its formation (Morbidelli et al., 2007; Walsh et al., 2011; Nesvorny and Morbidelli, 2012; Nesvorny, 2015a,b; Deienno et al., 2017; Gomes et al., 2017).

Because TNOs are generally faint, testing the outcomes of dynamical evolution models against the physical characteristics of TNOs is difficult. To get samples large enough to be statistically significant, surveys have been undertaken at various wavelengths and with different techniques so to constrain their:

- Colors (Fornasier et al., 2004a; Peixinho et al., 2004; Doressoundiram et al., 2005; DeMeo et al., 2009; Fraser and Brown, 2012; Perna et al., 2013; Schwamb, (in preparation)),
- Surface compositions (Barkume et al., 2008; Fornasier et al., 2009; Guilbert et al., 2009; Barucci et al., 2011; Brown, 2012), and
- Sizes and albedos (Stansberry et al., 2008; Mueller et al., 2009; Mommert et al., 2012; Santos-Sanz et al., 2012; Vilenius et al., 2012; Bauer et al., 2013; Lellouch et al., 2013, 2017).

The vast majority of TNOs are too faint for spectroscopic studies though, so most of our understanding of TNOs comes from broadband photometric surveys mentioned above (Brown et al., 2011b; Peixinho et al., 2012, 2015; Dalle Ore et al., 2013; Lacerda et al., 2014). TNOs show a vast variety of physical properties. For example, their albedo varies from a few percent to almost 100% for the largest objects, and colors vary from neutral-blue compared to the Sun to the reddest color observed in the solar system. Interpreting the observational dataset can be challenging and involves a detailed understanding of primordial properties of TNOs and evolutionary processes such as:

- Irradiation (Brunetto et al., 2006; Bennett et al., 2013; Poston et al., 2018),
- Volatile retention (Schaller and Brown, 2007a; Brown et al., 2011b; Wong and Brown, 2017),
- Differentiation and surface renewal (McKinnon et al., 2008; Guilbert-Lepoutre et al., 2011; Shchuko et al., 2014; Malamud and Prialnik, 2015), and
- Collisions (possibly disruptive; Barr and Schwamb, 2016),

There is a consensus over the fact that Cold Classicals stand out from the rest of TNOs due to their physical properties: redder colors and in general a specific surface type (Tegler and Romanishin, 2000; Pike et al., 2017), a large number of binaries with large separations (Noll et al., 2008a,b; Parker et al., 2011), higher albedos (Brucker et al., 2009; Vilenius et al., 2014), and a different size distribution (Bernstein et al., 2004; Fraser et al., 2010, 2014) lacking large objects (Levison and Stern, 2001). These TNOs are thought to have formed in place from material distinct from other TNOs in the disk, which were implanted from regions closer to the Sun than their current location. Centaurs (gravitationally-destabilized TNOs orbiting in the giant plant region) and small TNOs display a bimodal color distribution (Tegler and Romanishin, 1998; Peixinho et al., 2003, 2012, 2015; Tegler et al., 2003, 2016; Wong and Brown, 2017). More generally, TNO surfaces fall into two broad types: dark blue or bright red (Lacerda et al., 2014). We note that the red group itself could be sub-divided (Pike et al., 2017). These may be linked to different initial compositions. There is also a correlation between the color and the inclination of TNOs (Tegler and Romanishin, 2000; Hainaut and Delsanti, 2002; Trujillo and Brown, 2002; Doressoundiram et al., 2005; Peixinho et al., 2008, 2015). The inclination distribution in each color group suggests that these TNOs were formed from different populations of planetesimals in the disk, rather than having suffered from distinct evolution processes such as collisional resurfacing (Marsset et al., 2019).

As helpful as broadband photometry may be, it remains a proxy in terms of providing constraints of TNOs' surface composition. In this context, it is expected that the next generation of telescopes, such as the James Webb Space Telescope (JWST), will enable the study of TNOs with an unprecedented sensitivity, improving both the quality of our data and the sample of objects studied. A particularly good target for JWST will be the population of large and mid-sized TNOs, with which we can study evolutionary processes in great detail. In this paper, we present this

TABLE 1 | Physical properties of selected mid-sized TNOs.

Number	Name	H	Satellite	ρ [g.cm^{-3}]	D [km]	p_V [%]	Information on the surface
90377	Sedna	1.5	-		906^{+314}_{-258}	$41.0^{+39.3}_{-18.6}$	Class RR
					1420^{+110}_{-180}	$20.7^{+6.6}_{-2.9}$	H_2O, CH_4, C_2H_6?
225088	2007 OR_{10}	1.8	Yes		1280 ± 210	$13.9^{+5.7}_{-3.9}$	H_2O, CH_4? CH_3OH?
					1535^{+75}_{-225}	$8.9^{+3.1}_{-0.9}$	
90482	Orcus	2.2	Vanth	2.47 ± 0.89	917 ± 25	$23.1^{+1.8}_{-1.1}$	Class BB
				$1.65^{+0.35}_{-0.24}$	906 ± 72	23.0 ± 2.0	H_2O, NH_3? CH_4?
				$1.53^{+0.15}_{-0.13}$	910^{+50}_{-40}	$19.7^{+3.4}_{-2.8}$	NH_3:H_2O? NH_4^+?
							C_2H_6?
50000	Quaoar	2.4	Weywot	2.13 ± 0.29	1070 ± 38	$12.7^{+1.0}_{-0.9}$	Class RR
				1.99 ± 0.46	**1110 ± 5**	**10.9 ± 0.7**	H_2O, CH_4, C_2H_6,
				$<1.82 \pm 0.28$	**$>1138 \pm 25$**	**$<14.0 \pm 10.0$**	NH_3:H_2O? N_2? CO?
174567	Varda	3.2	Ilmarë	$1.27^{+0.41}_{-0.44}$	705^{+81}_{-75}	$10.2^{+2.4}_{-2.0}$	Class IR
				$1.24^{+0.50}_{-0.35}$	722^{+82}_{-76}	$16.6^{+4.3}_{-3.3}$	Inconclusive
55565	2002 AW_{197}	3.3	-		768^{+39}_{-38}	$11.2^{+1.2}_{-1.1}$	Class IR
					960^{+110}_{-180}	$9.4^{+4.7}_{-1.8}$	H_2O?
					742^{+98}_{-104}	$11.5^{+4.1}_{-2.5}$	
20000	Varuna	3.6	-	$0.99^{+0.86}_{-0.15}$	668^{+154}_{-86}	$12.7^{+4.0}_{-4.2}$	Class IR
					>670*	**>4***	H_2O?
					<1130*		
28978	Ixion	3.6	-		617^{+19}_{-20}	14.1 ± 1.1	Class IR, RR
					980^{+110}_{-180}	$9.9^{+4.8}_{-1.9}$	H_2O?
					650^{+260}_{-220}	$12.0^{+14.0}_{-6.0}$	
208996	2003 AZ_{84}	3.6	Yes	0.87 ± 0.01	724 ± 64	$10.7^{+2.3}_{-1.6}$	Class BB
					764 ± 6*	**9.7 ± 0.9***	H_2O, CH_3OH?
					692 ± 12*		
55637	2002 UX_{25}	3.6	Yes	0.80 ± 0.13	670 ± 34	$10.7^{+0.5}_{-0.8}$	Class IR, RR
				0.78 ± 0.10	659 ± 38	10.0 ± 1.0	Inconclusive
					695^{+30}_{-29}	$10.4^{+1.1}_{-1.0}$	
90568	2004 GV_9	4.0	-	1.14–1.19	680 ± 34	7.7 ± 0.8	Class BR, IR
					820^{+100}_{-170}	$6.8^{+4.0}_{-1.4}$	Inconclusive
					684^{+68}_{-74}	$7.3^{+4.9}_{-2.9}$	
120347	Salacia	4.1	Actaea	$1.29^{+0.29}_{-0.23}$	829 ± 30	4.4 ± 0.4	Class BB, BR
				1.26 ± 0.16	866 ± 37	4.2 ± 0.4	Inconclusive
				$1.16^{+0.59}_{-0.36}$			

*H values are from the JPL Solar System Database at http://ssd.jpl.nasa.gov. Diameters and albedos from the "TNOs are cool" key program on Herschel are given on a gray background for the primary in case of a multiple system (available at http://public-tnosarecool.lesia.obspm.fr/Published-results.html). Other measurements are also provided for comparison: values from stellar occultations are given in bold. *: Varuna and 2003 AZ_{84} may have a non-spherical shape, Varuna in particular has shown variable albedo, size and surface composition since it was first observed. Stellar occultations by 2003 AZ_{84} provide the following size: $(470 \pm 20) \times (383 \pm 10) \times (245 \pm 8)$ km (Dias-Oliveira et al., 2017), yielding an equivalent spherical radius of 383 ± 6 km, well within the thermal measurements (364 ± 33 km; Mommert et al., 2012). References can be found in **Table 3**.*

population in section Large and Mid-size TNOs, the telescope and in particular the NIRSpec instrument in section Overview of JWST/NIRSpec, as well as several studies and diagnotics to improve our understanding of TNO surface composition and evolution in section Observing Mid-sized TNOs with NIRSpec.

LARGE AND MID-SIZE TNOS

TNOs in general can trace not only the protoplanetary disk and the outcomes of planetary migrations, but also formation mechanisms and evolutionary processes which may have affected them to different degrees. For example, Barr and Schwamb (2016) suggest that two different types of collisions may explain the properties of large TNOs. Gentle collisions early enough in the history of TNOs (to avoid differentiation) would produce binary systems with medium densities and high mass ratios such as Pluto/Charon or Orcus/Vanth, whereas high-speed collisions onto differentiated objects would be the origin of high-density objects such as Quaoar/Weywot or Haumea and its collisional family. Therefore, a detailed knowledge of large and mid-size TNOs' physical properties (given in **Table 1** for mid-size TNOs, excluding the three largest members Pluto, Eris and Makemake) might allow us to use them as chronometers of events that occurred during the early stages of the solar system.

Irradiation Chemistry

The surface of atmosphereless objects is subject to long-term irradiation by solar wind, UV photons and cosmic rays capable of inducing changes in its chemical composition (Hudson et al., 2008). Long term irradiation of simple hydrocarbons leads to the breaking of C-H bonds, loss of H and formation longer C-chains: for example the continued irradiation of methane (CH_4) produces ethane (C_2H_6), ethylene (C_2H_4), acetylene (C_2H_2) and other higher mass alkanes. Understanding irradiation chemistry is crucial for understanding the nature and distribution of organics in the solar system, with direct implications for the chemistry of the solar nebula. For instance, the nature of the dark material that lowers the albedo of TNOs is still unknown. Organics are suspected to produce the reddest colors observed amongst TNOs, but the lack of high quality data for many objects has prevented a strong confirmation. These compounds, however, have different diagnostic absorption features beyond 3 microns, which will be accessible from NIRSpec. For example, Parker et al. (2016) presented hypothetical surface compositions for Sedna out to 5 microns, so far indistinguishable in the current dataset, which is limited mostly to < 2.5 microns.

Our greatest laboratories for studying irradiation chemistry may be Makemake, Quaoar and 2007 OR10. The surface of Makemake is dominated by methane. However, some deviations from the CH_4 spectrum have been identified as due to the presence of C_2H_6, then C_2H_2, C_2H_4 and propane (C_3H_8) (Brown et al., 2015; Lorenzi et al., 2015; Perna et al., 2017). Quaoar has a surface dominated by the presence of water ice, with significantly less coverage in methane than Makemake (Jewitt and Luu, 2004; Schaller and Brown, 2007b). However, its red color could be interpreted as due to the presence of irradiated hydrocarbons. Absorption features present in its near-infrared spectrum, in addition to water ice features, have revealed the presence of C_2H_6 in addition to CH_4 (Dalle Ore et al., 2009). Having similar physical properties, TNO 2007 OR10 is suspected of also displaying irradiated hydrocarbons (Brown et al., 2011a). While water ice absorption bands can be observed, a spectrum with a higher signal-to-noise ratio is required to confirm the presence of irradiation products on its surface.

Differentiation and Cryovolcanism

Cryovolcanism on mid-sized TNOs is an intriguing prospect, as these objects are generally deemed too small to sustain any geophysical activity. Models suggest that some TNOs may be differentiated owing to the right combination of size and density (Merk and Prialnik, 2006; McKinnon et al., 2008; Guilbert-Lepoutre et al., 2011; Shchuko et al., 2014; Malamud and Prialnik,

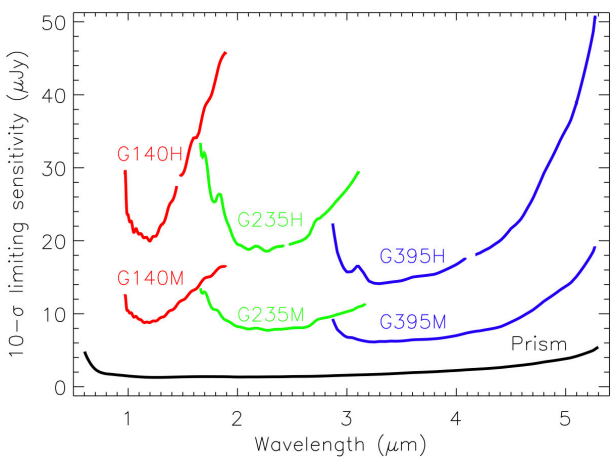

FIGURE 1 | Sensitivity limits (10-σ) for the NIRSpec integral field unit (IFU), with the various filter/grating combinations. The G140H and G140M gratings are shown for only the F100LP filter combination. This plot was created using the JWST Exposure Time Calculator (ETC) found at jwst.etc.stsci.edu and the following parameters: a point source with a flat continuum set to 10 μJy, the NRSIRS2RAPID readout mode, FULL frame subarray, 67 groups/1 integration/1 exposure (totaling 992 s of photon collection time), the "IFU Nod Off Scene" strategy, a 0.2" aperture radius, and a high background centered at (12^h, 0°).

TABLE 2 | Detailed observing strategy for the NIRSpec GTO of Orcus and 2003 AZ_{84}.

Target Acquisition: none
Observing Template: NIRSpec IFU Spectroscopy, 4-point-dither

Grating/Filter	Groups	Total Integration (s)
Orcus		
CLEAR/PRISM	20	1225.467
G140H/F100LP	25	1517.245
G235H/F170LP	30	1809.022
G395H/F290LP	60	3559.689

Target Acquisition: WATA, SUB2048, readout NRS
Observing Template: NIRSpec Fixed Slit Spectroscopy, S200A1, 3-point-dither

2003AZ_{84}		
CLEAR/PRISM	30	1356.767
G140M/F100LP	30	1356.767
G235M/F170LP	60	2669.767
G395M/F290LP	80	3545.100

TABLE 3 | References for TNO characteristics given in **Table 1**.

90377 Sedna	Lykawka and Mukai, 2005; Trujillo et al., 2005; Emery et al., 2007; Stansberry et al., 2008; Barucci et al., 2010; Lellouch et al., 2013; Braga-Ribas et al., 2014
225088 2007 OR_{10}	Tancredi, 2010; Brown et al., 2011a, 2012; Santos-Sanz et al., 2012; Pál et al., 2016; Holler et al., 2017; Kiss et al., 2017
90482 Orcus	Fornasier et al., 2004b, 2013; de Bergh et al., 2005; Lykawka and Mukai, 2005; Trujillo et al., 2005; Brown and Suer, 2007; Barucci et al., 2008; Stansberry et al., 2008; Delsanti et al., 2010; DeMeo et al., 2010; Carry et al., 2011; Thirouin et al., 2014; Brown and Butler, 2017, 2018; Kovalenko et al., 2017
50000 Quaoar	Brown and Trujillo, 2004; Jewitt and Luu, 2004; Lykawka and Mukai, 2005; Brown and Suer, 2007; Schaller and Brown, 2007b; Stansberry et al., 2008; Brucker et al., 2009; Dalle Ore et al., 2009; Guilbert et al., 2009; Fraser and Brown, 2010; Vachier et al., 2012; Braga-Ribas et al., 2013; Fornasier et al., 2013; Davis et al., 2014; Thirouin et al., 2014; Barucci et al., 2015; Brown and Butler, 2017; Kovalenko et al., 2017; Lellouch et al., 2017
174567 Varda	Barucci et al., 2011; Grundy et al., 2011, 2015; Brown et al., 2012; Thirouin et al., 2014; Vilenius et al., 2014; Souza-Feliciano et al., 2018
55565 2002 AW_{197}	Cruikshank et al., 2005; Doressoundiram et al., 2005; Grundy et al., 2005; Lykawka and Mukai, 2005; Barkume et al., 2008; Brucker et al., 2009; Guilbert et al., 2009; Merlin et al., 2010; Vilenius et al., 2014; Souza-Feliciano et al., 2018
20000 Varuna	Licandro et al., 2001; Grundy et al., 2005; Lykawka and Mukai, 2005; Lacerda and Jewitt, 2007; Barkume et al., 2008; Barucci et al., 2008; Brucker et al., 2009; Lellouch et al., 2013; Braga-Ribas et al., 2014; Lorenzi et al., 2014
28978 Ixion	Licandro et al., 2002; Boehnhardt et al., 2004; Grundy et al., 2005; Lykawka and Mukai, 2005; Barkume et al., 2008; Stansberry et al., 2008; Guilbert et al., 2009; Merlin et al., 2010; Trujillo et al., 2011; Lellouch et al., 2013; Souza-Feliciano et al., 2018
208996 2003 AZ_{84}	Lykawka and Mukai, 2005; Brown and Suer, 2007; Barkume et al., 2008; Stansberry et al., 2008; Guilbert et al., 2009; Merlin et al., 2010; Barucci et al., 2011; Mommert et al., 2012; Thirouin et al., 2014; Dias-Oliveira et al., 2017; Souza-Feliciano et al., 2018
55637 2002 UX_{25}	Lykawka and Mukai, 2005; Barkume et al., 2008; Brucker et al., 2009; Barucci et al., 2011; Brown et al., 2012; Fornasier et al., 2013; Vilenius et al., 2014; Brown and Butler, 2017; Kovalenko et al., 2017; Lellouch et al., 2017; Souza-Feliciano et al., 2018
90568 2004 GV_9	Lykawka and Mukai, 2005; Dotto et al., 2008; Brucker et al., 2009; Guilbert et al., 2009; Barucci et al., 2011; Brown et al., 2012; Vilenius et al., 2012; Souza-Feliciano et al., 2018
120347 Salacia	Noll et al., 2006; Schaller and Brown, 2008; Stansberry et al., 2012; Fornasier et al., 2013; Vilenius et al., 2014; Brown and Butler, 2017; Holler et al., 2017; Kovalenko et al., 2017; Lellouch et al., 2017

2015). In addition, the density of Haumea and Quaoar is best explained in a scenario where they suffered from a high-speed collision after they differentiated and had their icy mantle fragmented (Barr and Schwamb, 2016). From a spectroscopic point of view, however, it is not clear which species could be suggestive of past cryovolcanic activity. We highlight the following aspects:

- Crystalline water ice was first detected in abundance at the surface of Quaoar (Jewitt and Luu, 2004) then later seen on other TNOs. Since crystalline water ice is converted into amorphous water ice by solar radiation and galactic cosmic rays in several Myr (Mastrapa and Brown, 2006; Cook et al., 2007), its presence at the surface of TNOs has been suggested as evidence for recent resurfacing.
- Ammonia (NH_3) hydrates have been detected on the surface of Charon (Cook et al., 2007), and possibly Orcus (Delsanti et al., 2010). These hydrates should also be destroyed on timescales shorter than 1–50 Myr (Strazzulla and Palumbo, 1998). For Charon, no mechanism other than recent localized emplacement at the surface (due to the flow of ammonia-rich liquid water onto the surface) has been able to conclusively explain the observations (Cook et al., 2007; McKinnon et al., 2008; Desch et al., 2009).
- Flyby images of Pluto and Charon from NASA/*New Horizons* show evidence for a complex geology with diverse landforms, terrain ages, glacial flows, and tectonics. The latest models for Charon indicate that subsurface oceans may have been produced, and could explain features observed at the surface of the satellite (Desch, 2015; Desch and Neveu, 2017).

Probing the surface composition of a TNO using spectroscopy is observationally challenging. This is however important to pursue because it may lift some degeneracies existing among broadband color measurements (several compounds may be responsible for the same color). Although each large and mid-size TNOs may hold a unique orbital and physical history, studying the surface composition of this population as a whole allows exploration of different aspects of their formation and evolution. In addition, Brown (2012) suggests there may be an inherent change of surface composition for objects larger than 600–650 km, possibly due to different physical processes dominating their evolution. Therefore, studying not only the largest objects we observe today, but also smaller objects, is critical to assess how, and how much, each process may have modified objects as we observe them today.

OVERVIEW OF JWST/NIRSPEC

The James Webb Space Telescope (JWST) is a next generation space observatory and an international collaboration between the National Aeronautics and Space Administration (NASA), the European Space Agency (ESA), and the Canadian Space Agency (CSA). The primary mirror of JWST is composed of 18 hexagonal segments with a diameter of 6.5 m and a total light collecting area of 254,009 cm^2. JWST is set to begin science operations in the early 2020s with a nominal mission lifetime of 5 years and sufficient onboard fuel for a 10-year mission. The fuel is necessary to keep JWST in orbit around the Earth-Sun L2 point, ∼0.01 AU from Earth. Passive cooling

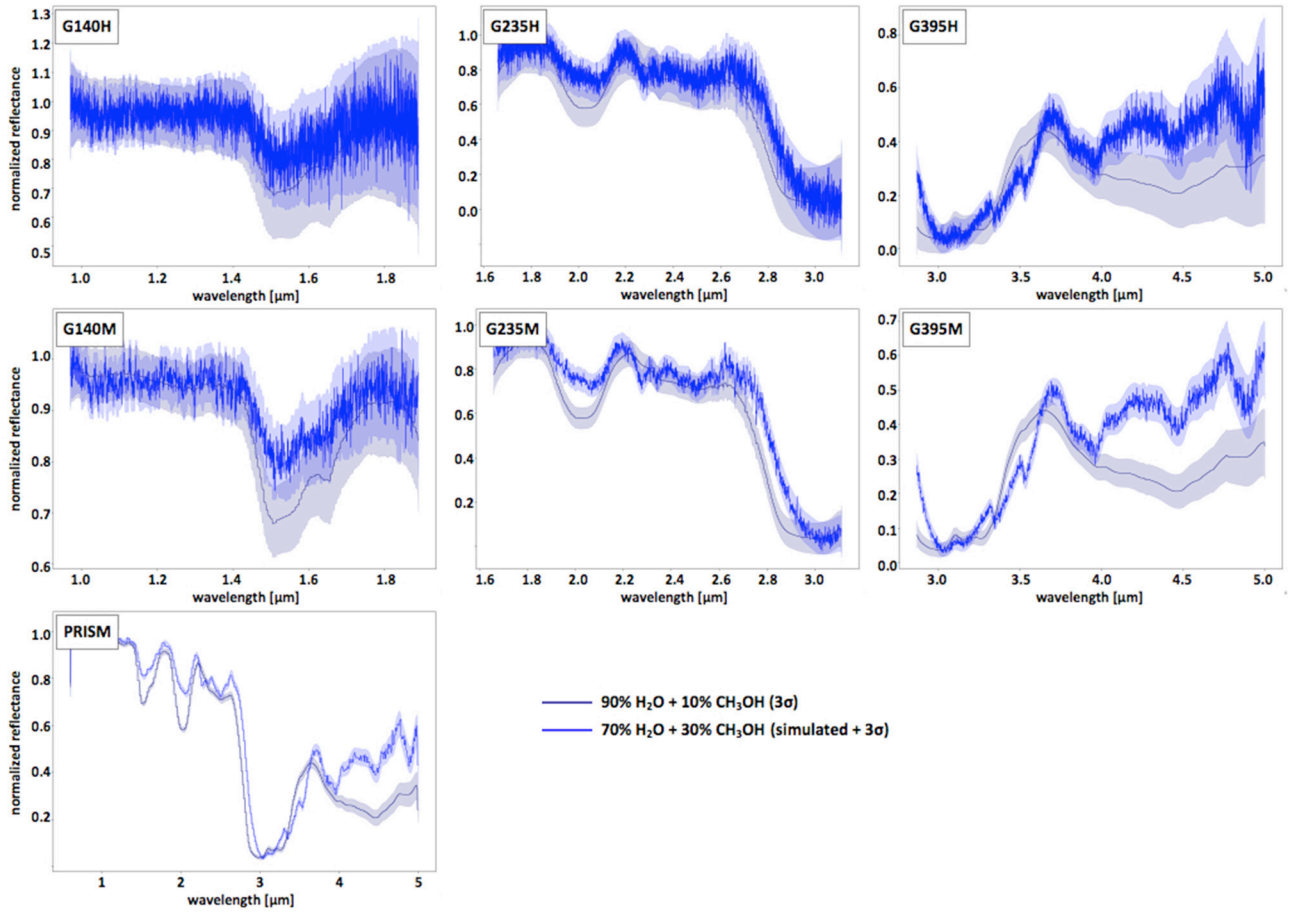

FIGURE 2 | Simulated spectra for two mixtures of water and methanol ice, shown (from top to bottom) for the high-, medium- and low-spectral resolution elements, respectively. The simulated signal is shown for one mixture for clarity. Shaded areas show the 3-σ detection limits corresponding to the simulated signal-to-noise ratios. Exposure time and other relevant instrumental features may be found in **Table 2**.

of the telescope will be handled by a large sunshield that must be directed at the Sun at all times. To maintain this thermal balance, JWST can only point in an allowable range of solar elongation angles (Sun-JWST-target angle) of 85–135°[1] This means that objects at opposition and objects interior to JWST's orbit (i.e., the Sun, Mercury, Venus, Earth, the Moon, and some near-Earth asteroids and long-period comets) cannot be observed at any time. These solar elongation constraints result in two observing windows symmetric about the Sun-JWST line, known as the "field of regard." For objects orbiting near the ecliptic plane, this results in two separate ∼50-day windows during which the object can be observed each year. In general, objects further from the ecliptic will be observable for longer periods of time, with a 5° region surrounding each ecliptic pole observable at all times. Faster-moving targets will be observable for shorter periods of time, but a majority of TNOs are moving slow enough that they can be considered effectively stationary. JWST will be commissioned to observe moving (solar system) targets starting at the beginning of science operations in Cycle 1. The maximum tracking rate is 30 mas/s, which corresponds to the maximum apparent rate for Mars, and so all TNOs will be observable for ∼100 days out of each year (Milam et al., 2016).

The JWST instrumentation consists of four science instruments and a guider known as the Fine Guidance Sensor (FGS). The science instruments are the Mid-Infrared Instrument (MIRI), the Near-Infrared Camera (NIRCam), the Near-Infrared Imager and Slitless Spectrograph (NIRISS), and the Near-Infrared Spectrograph (NIRSpec). This paper focuses on TNO observations with NIRSpec (e.g., Bagnasco et al., 2007), but additional information on all instruments can be found at the JWST User Documentation page (jwst-docs.stsci.edu). NIRSpec covers wavelengths from 0.6 to 5.3 μm at three different spectral resolutions. There are 7 different dispersers available: 3 high-resolution (R∼2,700) gratings (G140H, G235H, G395H), 3 medium-resolution (R∼1000) gratings (G140M, G235M, G395M), and one low-resolution (R∼30–300) prism (PRISM). To prevent order contamination, four long-pass filters (F070LP, F100LP, F170LP,

[1]https://jwst-docs.stsci.edu/display/JTI/JWST+Observatory+Coordinate+System+and+Field+of+Regard?q=field%20of%20regard.

F290LP) are used in conjunction with the medium- and high-resolution gratings; a CLEAR filter is used with the PRISM disperser, allowing the coverage of the full 0.6–5.3 μm spectral range at once.

The possible observing modes for TNO observations are the fixed slits and the integral field unit (IFU; Closs et al., 2008); all filter/grating combinations are available for use with these modes. In reality, due to uncertainties in the apparent positions of many TNOs (though most large- and mid-size TNOs have 1-year uncertainties >1 arcsec, nearly half of the TNOs in the MPC database have orbital uncertainties larger than 1 arcsec), blind pointing with the IFU will be the only option for spectral observations of the majority of them unless additional, more accurate astrometry using ground-based facilities becomes available in the time leading up to JWST science operations. The wide aperture target acquisition (WATA) available for accurate positioning of a target in the fixed slits or the IFU required to know the position of the target to better than 1" to be able to blindly position it in the 1.6" × 1.6" WATA aperture. Unfortunately, the standard target acquisition with micro-shutter arrays (MSA) that would have allowed to perform target acquisition using reference targets over a much larger field of view is not possible for moving targets.

While NIRSpec IFU observations are better-suited for TNOs with poorly-constrained orbits, the signal-to-noise ratio (SNR) of the spectra extracted from the IFU data cube will be lower than would be obtained for the same filter/grating strategy and total photon collection time with the fixed slits. After being processed through the pipeline the IFU data are in the form of a data cube: two spatial dimensions and one spectral dimension. This means there is an image for each wavelength "slice" rather than a single column in a fixed slit spectrum. More pixels must be extracted in each slice compared to each column in a fixed slit spectrum, resulting in elevated noise for the same amount of signal. This reduces the SNR for IFU observations of faint targets compared to fixed-slit observations by ∼30–40%, but this may be an unavoidable trade-off in order to observe the objects of interest with poorly constrained orbits. **Figure 1** presents the sensitivity limits for the IFU and the various filter/grating combinations.

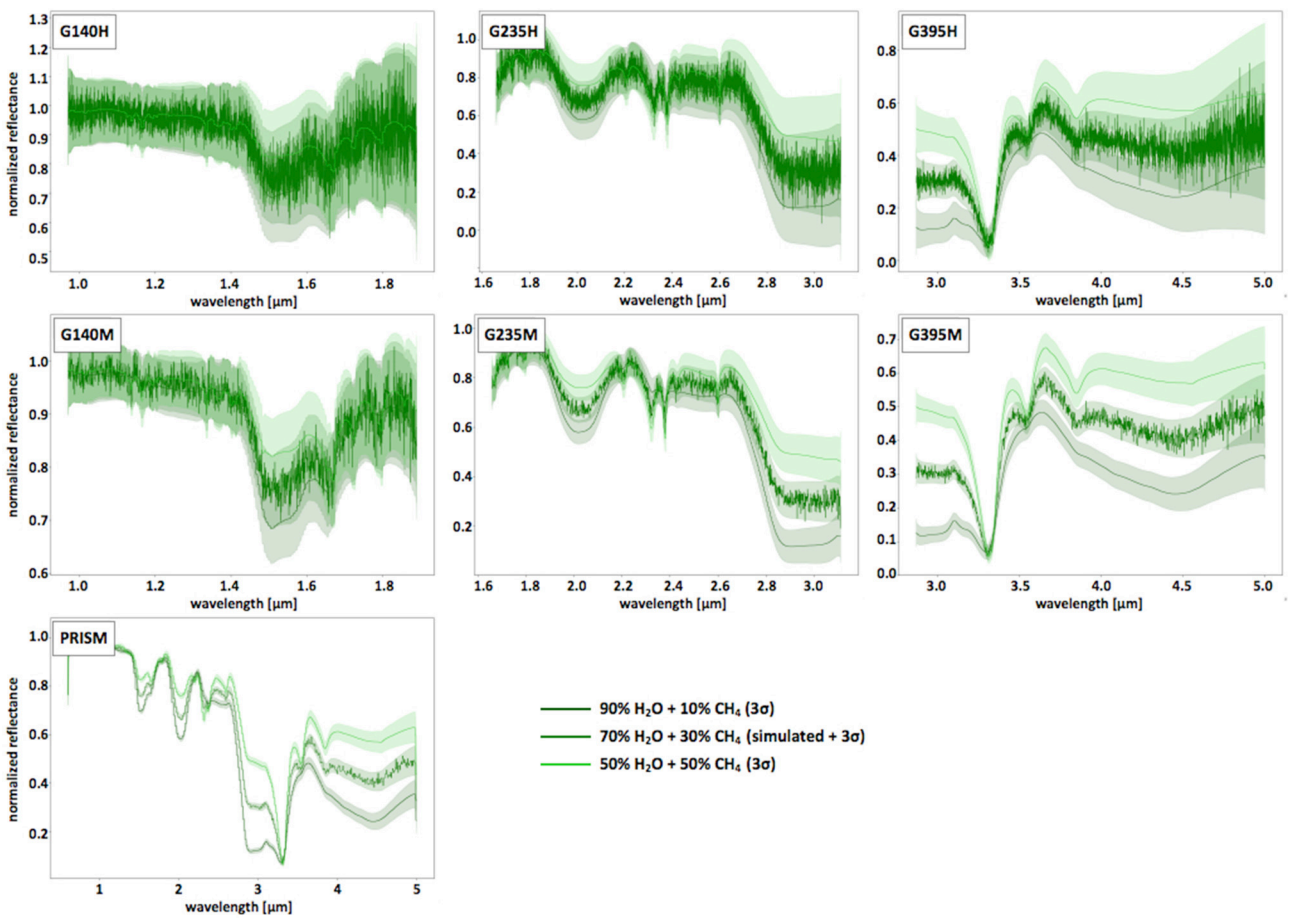

FIGURE 3 | Simulated spectra for two mixtures of water and methane ice, shown (from top to bottom) for the high-, medium- and low-spectral resolution elements, respectively. The simulated signal is show for one mixture for clarity. Shaded areas shown the 3-σ detection limits corresponding to the simulated signal-to-noise ratios. Exposure time and other relevant instrumental features may be found in **Table 2**.

OBSERVING MID-SIZED TNOS WITH NIRSPEC

NIRSpec Guaranteed Time Observations (GTO) of TNOs

GTO were granted through several channels, and several programs will be dedicated to the observation of TNOs (see the complete list at: https://jwst.stsci.edu/observing-programs/approved-gto-programs). The NIRSpec team has set aside time for a small program focused on two mid-sized TNOs: Plutinos Orcus and 2003 AZ_{84}. We thus briefly detail this program (**Table 2**): because of the flux difference between both objects, the observing strategy we chose for each is different. Orcus will be observed with the integral-field unit (IFU) mode of NIRSpec. It is also bright enough that we can use the high-spectral resolution configurations covering the 1.0–5.2 micron range without dramatically increasing the total observing time. Given that this object has accurate astrometry and in order to minimize the overheads, we have decided to use a point-and-shoot strategy (no target acquisition) and a 4-point nodding pattern. Because it is fainter, 2003 AZ_{84} will be observed with a slit and at medium-spectral resolution configurations with a 3-point nodding pattern. For both objects, the low-resolution configuration (PRISM) will also be used, as it can cover the 0.6–5.3 micron range in one shot. For all observations, the readout pattern will be set to NRSIRS2RAPID to reduce the detector noise and retrieve all the individual readouts. All exposures are specified with a single integration. In the following, we use the settings selected for Orcus as a reference point to illustrate mid-sized TNO spectra. This will allow us to assess the performance of NIRSpec by comparing the TNO spectra once the objects are actually observed.

Ice Mixtures Relevant to Mid-sized TNO Observations

Based on data collected from the ground (**Table 1**), we see that the surface spectrum of mid-sized TNOs is dominated by water ice, with a few additional ice species present in addition, like ammonia, methane, ethane or methanol, though some of these other species may be more difficult to detect. We aim to make

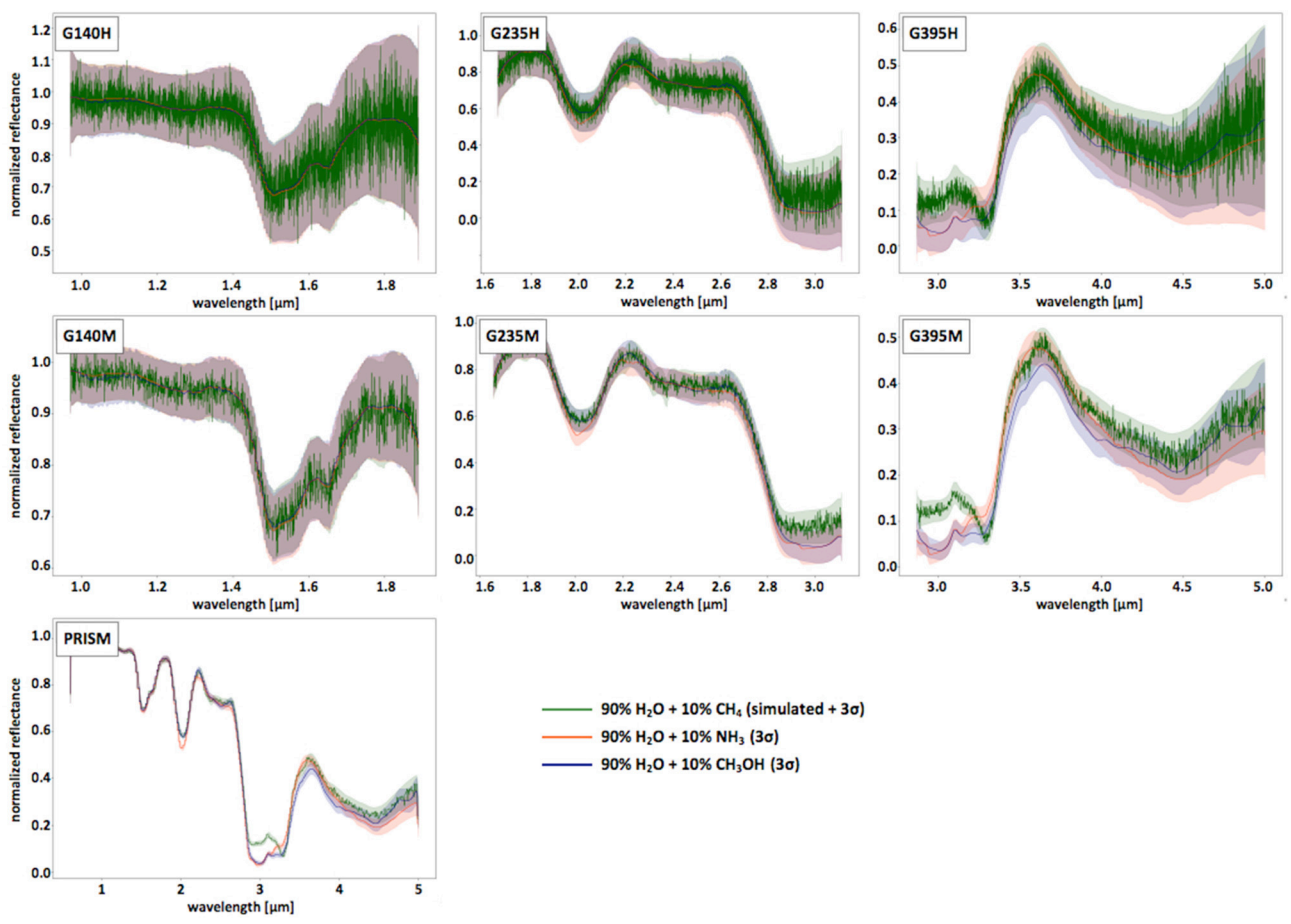

FIGURE 4 | Simulated spectra for mixtures of 90% water ice with 10% of methane, ammonia, and methanol ice, shown (from top to bottom) for the high-, medium- and low-spectral resolution elements, respectively. The simulated signal is shown for one mixture for clarity. Shaded areas show the 3-σ detection limits corresponding to the simulated signal-to-noise ratios. Exposure time and other relevant instrumental features may be found in **Table 2**.

first order assessments of the performance of NIRSpec, so we use mixtures of two or three of these components to compute reflectance spectra of typical mid-size TNOs: typically water ice plus one or two of the following components: methane, ammonia, methanol. We then use the radiative transfer model of Hapke (1981, 1993) with optical constants of those components to produce synthetic spectra of typical mixtures. We use the water-ice optical constants from Clark et al. (2012), and optical constants from the GhoSST database (now part of the SSHADE database; Schmitt et al., 2018) for the other species (https://ghosst.osug.fr, https://www.sshade.eu). At this stage, we do not include any dust or reddening component. These would not change the position of the absorption features, only their depths due to the relative amount of each compound in the mixture.

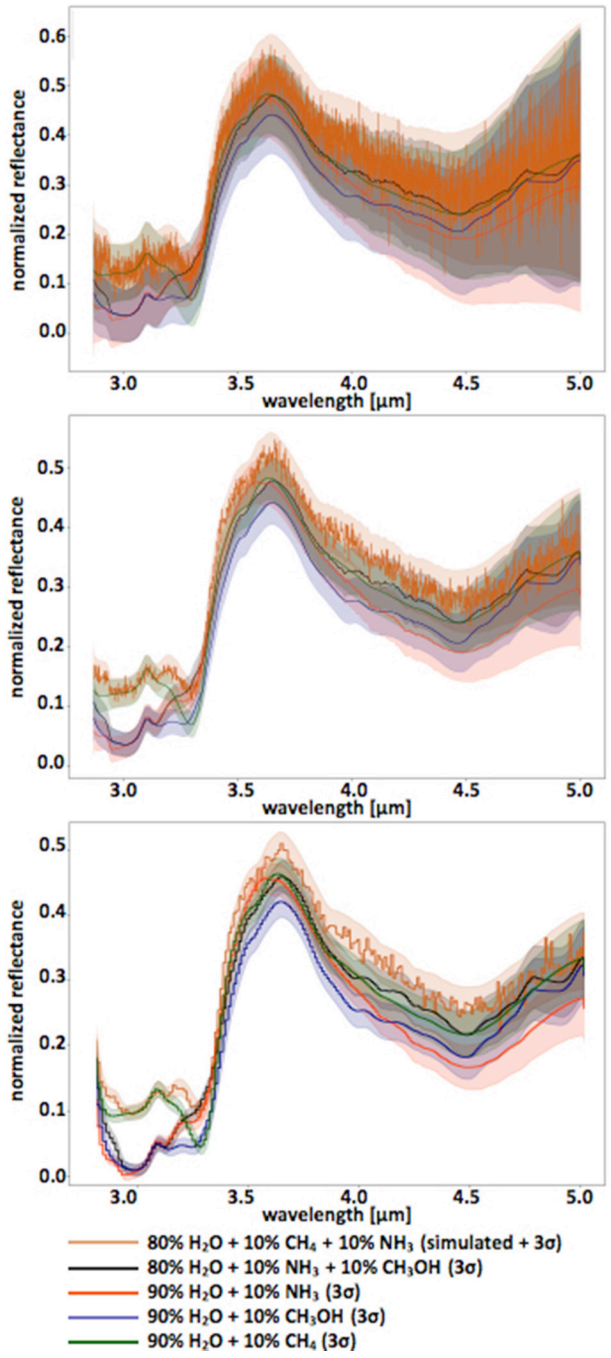

FIGURE 5 | Simulated spectra for various ice mixtures relevant to mid-sized TNO surface compositions (water as themajor ice species with contributions from methane, ammonia and methanol ice), focused on the 3–5 micron wavelength range, for high-, medium-, and low-spectral resolution (from top to bottom, respectively). The simulated signal is shown for one mixture only for clarity. Shaded areas show the 3-σ detection limits corresponding to the simulated signal-to-noise ratios.

RESULTS

The synthetic spectra obtained for ideal mixtures of ices are convolved with the spectrum of a solar analog in order to simulate the reflectance of a TNO surface. These are then normalized to various magnitudes typical of mid-sized TNOs: **Figures 2**–**5** below show the spectra for a J-magnitude of 18.2. We use the resulting spectra as input to simulate the signal received by the detector and the corresponding noise, using the various instrumental features such as readout pattern or spectral elements relevant to the observations. We stress again that in the following, we use the relatively short exposure times selected for Orcus in the NIRSpec GTO program, given in **Table 2**. Our results were tested against the official JWST Exposure Time Calculator (ETC) and were found to agree with the ETC results to typically better than ±10%.

Figures 2, **3** show examples of simulated spectra corresponding to mixtures of water and methanol ice (9:1 and 7:3) and water and methane ice (9:1, 7:3, and 5:5), using from top to bottom the high-spectral resolution, medium-spectral resolution (exposure times equal to those used for the high-spectral resolution, see **Table 2** for Orcus), and low-spectral resolution options. It is obvious in these examples that the lower the spectral resolution, the higher the SNR. As for data obtained from the ground, higher SNRs can be achieved with the high-spectral resolution by binning the data and thus artificially lowering the effective spectral resolution. However, most of the time, NIRSpec observations of faint targets are detector-noise dominated so the SNR after binning will be lower than one that would be obtained for direct observations at lower spectral resolution. The advantage of having a high spectral resolution is that it allows for the investigation of the dilution degree and phase properties of ices, and provides accurate thermometry of the surface (see Merlin et al., 2018, for example). **Figure 4** shows a comparison between mixtures of 90% water ice and 10% of one of the other ice we considered: methane, ammonia and methanol, which are best disentangled around 3 microns.

One interesting point to note is that the lowest spectral resolution when using the PRISM falls in the 1.0–1.4 micron wavelength range, and increases toward longer wavelengths. Therefore, we can expect to reach a resolving power >100 in the 3–5 micron range, where the molecules expected to be present at the surface of TNOs show their fundamental vibration bands and are best disentangled. A comparison between the

three spectral resolutions in the 3–5 micron range is shown in **Figure 5**, where the exposure times for the high- and medium-spectral resolutions is 3,560 s for the G395H and G395M gratings, respectively, which corresponds to roughly three times the exposure time used for the PRISM (1225s). The mixtures used for this figure include 5 mixtures of water ice with one or two other compounds. We see that the absorption features around 3 microns are best separated (at more than 3-σ) with the low resolution.

DISCUSSION

From the ground, the variety of chemical compounds present at the surface of TNOs have been detected through the overtones and combination bands of O-H, C-H and N-H bounds up to 2.5 microns. NIRSpec is expected to open a new window into our understanding of TNO surface composition through the identification of their fundamental absorption bands in the 3–5 micron region. We simulated TNO spectra observed by JWST/NIRSpec using ideal mixtures of ices, without any dust or coloring compound that would change the depths of absorption features compared to the results we have shown. We have seen that for an object with a J-magnitude similar to Orcus' and relatively small exposures, the SNRs achieved for most TNOs' brightness will be sufficient to detect shallow absorption bands corresponding to 5–10% of ice at the surface. We argue that the key aspect to advance our understanding of TNO surface composition will be related to the spectral resolution. Obviously, the highest spectral resolution will address the unexpected: molecules we may not anticipate, dilution and ice phases, as well as a detailed investigation of the surface temperature. This aspect will be tested with the GTO observations of Orcus.

This is however expensive, even for bright objects like Orcus (whose surface composition is already well constrained from the ground). From our experience of preparing multiple observations, we see that the efficiency of NIRSpec observations of solar system moving targets is typically 50–60%. Therefore, achieving a high SNR as well as a high spectral resolution may lead to very long observing programs that may prove difficult to get through a time allocation committee.

The medium spectral resolution may be an alternative strategy: we see that we typically achieve higher SNRs when using the same exposure times as for the high spectral resolution. Using slits instead of the IFU will also allow an increase of the SNR. This will be tested with the GTO observations of 2003 AZ_{84}, for which both slits and medium-spectral resolutions will be used. In addition, the PRISM mode will be used for both objects and will allow direct comparison of the results achieved by the different spectral resolution modes.

From our simulations, we anticipate that an efficient strategy may be to systematically observe the objects with the PRISM mode in order to get the full spectral coverage in one shot and with a good SNR. This will already allow the disentanglement of most species expected at the surface of TNOs. Then, instead of adding high-spectral resolution observations for the complete wavelength range, observations could be limited to the G395M or G395H gratings (medium- or high-spectral resolution) that cover the key 3–5 micron wavelength range). This combination of spectral configurations appears very promising on paper, for detailed investigations of the physical nature of components present at the surface of TNOs. The NIRSpec GTO program on Orcus and 2003 AZ_{84} will provide an early, real-life test of this strategy.

AUTHOR CONTRIBUTIONS

RM: review, biblio, writing. AG-L: review, biblio, writing, methods, supervision. PF: simulations, writing, methods. FM: input data, writing. BH: writing, methods. NC: biblio, writing. CQ-N: biblio, supervision.

FUNDING

The fees will be paid by CNRS credits given to the UTINAM institute as part of the regular funding of institutions in France. This project has received partial funding from the European Research Council (ERC) under grant agreement No 802699.

ACKNOWLEDGMENTS

RM is grateful to the ESTEC Faculty Council for funding. We are thankful to referees for their useful comments which improved the quality of this manuscript.

REFERENCES

Bagnasco, G., Kolm, M., Ferruit, P., Honnen, K., Koehler, J., Lemke, R., et al. (2007). Overview of the near-infrared spectrograph (NIRSpec) instrument on-board the James Webb Space Telescope (JWST). *SPIE* 6692:66920M. doi: 10.1117/12.735602

Barkume, K. M., Brown, M. E., and Schaller, E. L. (2008). Near-infrared spectra of centaurs and kuiper belt objects. *Astronomic. J.* 135, 55–67. doi: 10.1088/0004-6256/135/1/55

Barr, A. C., and Schwamb, M. E. (2016). Interpreting the densities of the Kuiper belt's dwarf planets. *Monthly Notices RAS* 460, 1542–1548. doi: 10.1093/mnras/stw1052

Barucci, M. A., Alvarez-Candal, A., Merlin, F., Belskaya, I. N., de Bergh, C., Perna, D., et al. (2011). New insights on ices in Centaur and Transneptunian populations. *Icarus* 214, 297–307. doi: 10.1016/j.icarus.2011.04.019

Barucci, M. A., Dalle Ore, C. M., Perna, D., Cruikshank, D. P., Doressoundiram, A., Alvarez-Candal, A., et al. (2015). (50000) Quaoaor: Surface composition variability. *Astron. Astrophys.* 584:107. doi: 10.1051/0004-6361/201526119

Barucci, M. A., Merlin, F., Guilbert, A., de Bergh, C., Alvarez-Candal, A., Hainaut, O., et al. (2008). Surface composition and temperature of the TNO Orcus. *Astron. Astrophys.* 479, 13–16. doi: 10.1051/0004-6361:20079079

Barucci, M. A., Morea Dalle Ore, C., Alvarez-Candal, A., de Bergh, C., Merlin, F., Dumas, C., et al. (2010). (90377) Sedna: investigation of surface compositional variation. *Astronom. J.* 140, 2095–2100. doi: 10.1088/0004-6256/140/6/2095

Bauer, J. M., Grav, T., Blauvelt, E., Mainzer, A. K., Masiero, J. R., Stevenson, R., et al. (2013). Centaurs and scattered disk objects in the thermal infrared: analysis of WISE/NEOWISE observations. *Astrophys. J.* 773:22. doi: 10.1088/0004-637X/773/1/22

Bennett, C. J., Pirim, C., and Orlando, T. M. (2013). Space-weathering of solar system bodies: a laboratory perspective. *Chem. Rev.* 113, 9086–9150. doi: 10.1021/cr400153k

Bernstein, G. M., Trilling, D. E., Allen, R. L., Brown, M. E., Holman, M., and Malhotra, R. (2004). The size distribution of trans-neptunian bodies. *Astronom. J.* 128, 1364–1390. doi: 10.1086/422919

Boehnhardt, H., Bagnulo, S., Muinonen, K., Barucci, M. A., Kolokolova, L., Dotto, E., et al. (2004). Surface characterization of 28978 Ixion (2001 KX76). *Astronomy Astrophys.* 415:21. doi: 10.1051/0004-6361:20040005

Braga-Ribas, F., Sicardy, B., Ortiz, J. L., Lellouch, E., Tancredi, G., Lecacheux, J., et al. (2013). The size, shape, albedo, density and atmospheric limit of transneptunian object (50000) Quaoar from multi-chord stellar occultations. *Astrophys. J.* 773, 1–13. doi: 10.1088/0004-637X/773/1/26

Braga-Ribas, F., Vieira-Martins, R., Assafin, M., Camargo, J. I. B., Sicardy, B., and Ortiz, J. L. (2014). "Stellar occultations by transneptunian and centaurs objects: results from more than 10 observed events," in *XIV Latin American Regional IAU Meeting*, eds A. Mateus, J. Gregorio-Hetem and R. Cid Fernandes (Florianópolis), 3.

Brown, M. E. (2012). The Compositions of Kuiper Belt Objects. *AREPS* 40, 476–494. doi: 10.1146/annurev-earth-042711-105352

Brown, M. E., Burgasser, A. J., and Fraser, W. C. (2011a). The surface composition of large kuiper belt object 2007 OR10. *Astrophys. J. Lett.* 738:26. doi: 10.1088/2041-8205/738/2/L26

Brown, M. E., and Butler, B. J. (2017). The density of mid-sized kuiper belt objects from ALMA thermal observations. *Astronom. J.* 154:19. doi: 10.3847/1538-3881/aa6346

Brown, M. E., and Butler, B. J. (2018). Medium-sized satellites of large Kuiper belt objects. *Astronom. J.* eprint arXiv:1801.07221.

Brown, M. E., Schaller, E. L., and Blake, G. A. (2015). Irradiation products on dwarf planet makemake. *Astronom. J.* 149:105. doi: 10.1088/0004-6256/149/3/105

Brown, M. E., Schaller, E. L., and Fraser, W. C. (2011b). A hypothesis for the color diversity of the kuiper belt. *Astrophys. J. Lett.* 739:60. doi: 10.1088/2041-8205/739/2/L60

Brown, M. E., Schaller, E. L., and Fraser, W. C. (2012). Water ice in the kuiper belt. *Astronom. J.* 143:146. doi: 10.1088/0004-6256/143/6/146

Brown, M. E., and Suer, T.-A. (2007). *IAU Circ. 8812, Satellites of 2003 AZ84, (50000), (55637) and (90482).* Available online at: http://adsabs.harvard.edu/abs/2007IAUC.8812....1B

Brown, M. E., and Trujillo, C. A. (2004). Direct measurements of the size of the large Kuiper Belt Object (50000) Quaoar. *Astronom. J.* 127:2413. doi: 10.1086/382513

Brucker, M. J., Grundy, W. M., Stansberry, J. A., Spencer, J. R., Sheppard, S. S., Chiang, E. I., et al. (2009). High albedos of low inclination Classical Kuiper belt objects. *Icarus* 201, 284–294. doi: 10.1016/j.icarus.2008.12.040

Brunetto, R., Barucci, M. A., Dotto, E., and Strazzulla, G. (2006). Ion irradiation of frozen methanol, methane, and benzene: linking to the colors of centaurs and trans-neptunian objects. *Astrophys. J.* 644, 646–650. doi: 10.1086/503359

Carry, B., Hestroffer, D., DeMeo, F. E., Thirouin, A., Berthier, J., Lacerda, P., et al. (2011). Integral-field spectroscopy of (90482) Orcus-Vanth. *Astron. Astrophys.* 534:A115. doi: 10.1051/0004-6361/201117486

Clark, R. N., Cruikshank, D. P., Jaumann, R., Brown, R. H., Stephan, K., Dalle Ore, C. M., et al. (2012). The surface composition of Iapetus: Mapping results from Cassini VIMS. *Icarus* 218, 831–860. doi: 10.1016/j.icarus.2012.01.008

Closs, M. F., Ferruit, P., Lobb, D. R., Preuss, W. R., Rolt, S., and Talbot, R. G. (2008). The integral field unit on the James Webb Space Telescope's Near-Infrared Spectrograph. *SPIE* 7010:701011. doi: 10.1117/12.788820

Cook, J. C., Desch, S. J., Roush, T. L., Trujillo, C. A., and Geballe, T. R. (2007). Near-infrared spectroscopy of charon: possible evidence for cryovolcanism on kuiper belt objects. *Astrophys. J.* 663, 1406–1419. doi: 10.1086/518222

Cruikshank, D. P., Stansberry, J. A., Emery, J. P., Fernández, Y. R., Werner, M. W., Trilling, D. E., et al. (2005). The high-albedo Kuiper Belt Object (55565) 2002 AW197. *Astrophys. J.* 624: 53. doi: 10.1086/430420

Dalle Ore, C.;, Barucci, M. A., Emery, J. P., Cruikshank, D. P., Dalle Ore, L. V., Merlin, F., et al. (2009). Composition of KBO (50000) Quaoar. *Astron. Astrophys.* 501, 349–357. doi: 10.1051/0004-6361/200911752

Dalle Ore, C. M., Dalle Ore, L. V., Roush, T. L., Cruikshank, D. P., Emery, J. P., Pinilla-Alonso, N., et al. (2013). A compositional interpretation of trans-neptunian objects taxonomies. *Icarus* 222, 307–322. doi: 10.1016/j.icarus.2012.11.015

Davis, A. B., Pasachoff, J. M., Babcock, B., Person, M. J., Zuluaga, C.A. Bosh, A. S., et al. (2014). *Observation and Analysis of a Single-Chord Stellar Occultation by Kuiper Belt Object (50000) Quaoar.* Available online at: http://adsabs.harvard.edu/abs/2014AAS...22324708D

de Bergh, C., Delsanti, A., Tozzi, G. P., Dotto, E., Doressoundiram, A., and Barucci, M. A. (2005). The surface of the transneptunian object 90482 Orcus. *Astron Astrophys.* 437, 1115–1120. doi: 10.1051/0004-6361:20042533

Deienno, R., Morbidelli, A., Gomes, R. S., and Nesvorny, D. (2017). Constraining the giant planets' initial configuration from their evolution: implications for the timing of the planetary instability. *Astronom. J.* 153:153. doi: 10.3847/1538-3881/aa5eaa

Delsanti, A., Merlin, F., Guilbert-Lepoutre, A., Bauer, J., Yang, B., and Meech, K. J. (2010). Methane, ammonia, and their irradiation products at the surface of an intermediate-size KBO? A portrait of Plutino (90482) Orcus. *Astron. Astrophys.* 520:A40. doi: 10.1051/0004-6361/201014296

DeMeo, F. E., Barucci, M. A., Merlin, F., Guilbert-Lepoutre, A., Alvarez-Candal, A., Delsanti, A., et al. (2010). A spectroscopic analysis of Jupiter-coupled object (52872) Okyrhoe, and TNOs (90482) Orcus and (73480) 2002 PN34. *Astron. Astrophys.* 521, 1–9. doi: 10.1051/0004-6361/201014042

DeMeo, F. E., Fornasier, S., Barucci, M. A., Perna, D., Protopapa, S., Alvarez-Candal, A., et al. (2009). Visible and near-infrared colors of Transneptunian objects and Centaurs from the second ESO large program. *Astron. Astrophys.* 493, 283–290. doi: 10.1051/0004-6361:200810561

Desch, S. J. (2015). Density of Charon formed from a disk generated by the impact of partially differentiated bodies. *Icarus* 246, 37–47. doi: 10.1016/j.icarus.2014.07.034

Desch, S. J., Cook, J. C., Doggett, T. C., and Porter, S. B. (2009). Thermal evolution of Kuiper belt objects, with implications for cryovolcanism. *Icarus* 202, 694–714. doi: 10.1016/j.icarus.2009.03.009

Desch, S. J., and Neveu, M. (2017). Differentiation and cryovolcanism on Charon: a view before and after New Horizons. *Icarus* 287, 175–186. doi: 10.1016/j.icarus.2016.11.037

Dias-Oliveira, A., Sicardy, B., Ortiz, J. L., Braga-Ribas, F., Leiva, R., Vieira-Martins, R., et al. (2017). Study of the Plutino Object (208996) 2003 AZ84 from Stellar occultations: size, shape, and topographic features. *Astronom. J.* 154:22. doi: 10.3847/1538-3881/aa74e9

Dodson-Robinson, S. E., Willacy, K., Bodenheimer, P., Turner, N. J., and Beichman, C. A. (2009). Ice lines, planetesimal composition and solid surface density in the solar nebula. *Icarus* 200, 672–693. doi: 10.1016/j.icarus.2008.11.023

Doressoundiram, A., Peixinho, N., Doucet, C., Mousis, O., Barucci, M. A., Petit, J. M., et al. (2005). The meudon multicolor survey (2MS) of Centaurs and trans-neptunian objects: extended dataset and status on the correlations reported. *Icarus* 174, 90–104. doi: 10.1016/j.icarus.2004.09.009

Dotto, E., Perna, D., Barucci, M. A., Rossi, A., de Bergh, C., Doressoundiram, A., et al. (2008). Rotational properties of centaurs and transneptunian objects. lightcurves and densities. *Astron. Astrophys.* 490, 829–833. doi: 10.1051/0004-6361:200809615

Emery, J. P., Dalle Ore, C. M., Cruikshank, D. P., Fernández, Y. R., Trilling, D. E., and Stansberry, J. A. (2007). Ices on (90377) Sedna: confirmation and compositional constraints. *Astron. Astrophys.* 466, 395–398. doi: 10.1051/0004-6361:20067021

Fornasier, S., Barucci, M. A., de Bergh, C., Alvarez-Candal, A., DeMeo, F., Merlin, F., et al. (2009). Visible spectroscopy of the new ESO large programme on trans-Neptunian objects and Centaurs: final results. *Astron. Astrophys.* 508, 457–465. doi: 10.1051/0004-6361/200912582

Fornasier, S., Doressoundiram, A., Tozzi, G. P., Barucci, M. A., Boehnhardt, H., de Bergh, C., et al. (2004a). ESO large program on physical studies of Transneptunian objects and Centaurs: final results of the visible spectrophotometric observations. *Astron. Astrophys.* 421, 353–363. doi: 10.1051/0004-6361:20041221

Fornasier, S., Dotto, E., Barucci, M. A., and Barbieri, C. (2004b). Water ice on the surface of the large TNO 2004 DW. *Astron. Astrophys.* 422, L43–L46. doi: 10.1051/0004-6361:20048004

Fornasier, S., Lellouch, E., Müller, T., Santos-Sanz, P., Panuzzo, P., Kiss, C., et al. (2013). TNOs are Cool: a survey of the trans-neptunian region. VIII. Combined Herschel PACS and SPIRE observations of nine bright targets at 70-500 μm. *Astron. Astrophys.* 555:A15. doi: 10.1051/0004-6361/201321329

Fraser, W. C., and Brown, M. E. (2010). Quaoar: a rock in the Kuiper Belt. *Astrophys. J.* 714, 1547–1550. doi: 10.1088/0004-637X/714/2/1547

Fraser, W. C., and Brown, M. E. (2012). The hubble wide field camera 3 test of surfaces in the outer solar system: the compositional classes of the kuiper belt. *Astrophys. J.* 749:33. doi: 10.1088/0004-637X/749/1/33

Fraser, W. C., Brown, M. E., Morbidelli, A., Parker, A., and Batygin, K. (2014). The absolute magnitude distribution of kuiper belt objects. *Astrophys. J.* 782:100. doi: 10.1088/0004-637X/782/2/100

Fraser, W. C., Brown, M. E., and Schwamb, M. E. (2010). The luminosity function of the hot and cold Kuiper belt populations. *Icarus* 210, 944–955. doi: 10.1016/j.icarus.2010.08.001

Gladman, B., Marsden, B. G., and Vanlaerhoven, C. (2008). "Nomenclature in the outer solar system," in *The Solar System Beyond Neptune,* eds M. A. Barucci, H. Boehnhardt, D. P. Cruikshank, and A. Morbidelli (Tucson: University of Arizona Press), 43–57.

Gomes, R., Deienno, R., and Morbidelli, A. (2017). The inclination of the planetary system relative to the solar equator may be explained by the presence of planet 9. *Astronom. J.* 153:27. doi: 10.3847/1538-3881/153/1/27

Gomes, R., Levison, H. F., Tsiganis, K., and Morbidelli, A. (2005). Origin of the cataclysmic Late Heavy Bombardment period of the terrestrial planets. *Nature* 435, 466–469. doi: 10.1038/nature03676

Grundy, W. M., Buie, M. W., and Spencer, J. R. (2005). Near-infrared spectrum of low-inclination Classical Kuiper Belt Object (79360) 1997 CS_{29}. *Astronom. J.* 130:1299. doi: 10.1086/431958

Grundy, W. M., Noll, K. S., Nimmo, F., Roe, H. G., Buie, M. W., Porter, S. B., et al. (2011). Five new and three improved mutual orbits of transneptunian binaries. *Icarus* 213:678. doi: 10.1016/j.icarus.2011.03.012

Grundy, W. M., Porter, S. B., Benecchi, S. D., Roe, H. G., Noll, K. S., Trujillo, C. A., et al. (2015). The mutual orbit, mass, and density of the large transneptunian binary system Varda and Ilmarë. *Icarus* 257, 130–138. doi: 10.1016/j.icarus.2015.04.036

Guilbert, A., Alvarez-Candal, A., Merlin, F., Barucci, M. A., Dumas, C., de Bergh, C., et al. (2009). ESO-large program on TNOs: near-infrared spectroscopy with SINFONI. *Icarus* 201, 272–283. doi: 10.1016/j.icarus.2008.12.023

Guilbert-Lepoutre, A., Lasue, J., Federico, C., Coradini, A., Orosei, R., and Rosenberg, E. D. (2011). New 3D thermal evolution model for icy bodies application to trans-Neptunian objects. *Astron. Astrophys.* 529:71. doi: 10.1051/0004-6361/201014194

Hainaut, O. R., and Delsanti, A. C. (2002). Colors of minor bodies in the outer solar system. A statistical analysis. *Astron. Astrophys.* 389, 641–664. doi: 10.1051/0004-6361:20020431

Hapke, B. (1981). Bidirectional reflectance spectroscopy. 1. Theory. *J. Geophys. Res.* 86, 4571–4586.

Hapke, B. (1993). *Theory of Reflectance and Emittance Spectroscopy*. Cambridge University Press. Available online at: https://www.cambridge.org/core/books/theory-of-reflectance-and-emittance-spectroscopy/C266E1164D5E14DA18141F03D0E0EAB0#

Holler, B. J., Young, L. A., Buie, M. W., Grundy, W. M., Lyke, J. E., Young, E. F., et al. (2017). Measuring temperature and ammonia hydrate ice on Charon in 2015 from Keck/OSIRIS spectra. *Icarus* 284, 394–406. doi: 10.1016/j.icarus.2016.12.003

Hudson, R. L., Palumbo, M. E., Strazzulla, G., Moore, M. H., Cooper, J. F., and Sturner, S. J. (2008). "Laboratory studies of the chemistry of transneptunian object surface materials," in *The Solar System Beyond Neptune,* eds M. A. Barucci, H. Boehnhardt, D. P. Cruikshank, and A. Morbidelli (Tucson: University of Arizona Press), 592, 507–523.

Jewitt, D. (2015). Color systematics of comets and related bodies. *Astronom. J.* 150:201. doi: 10.1088/0004-6256/150/6/201

Jewitt, D., and Luu, J. (1993). Discovery of the candidate Kuiper belt object 1992 QB1. *Nature* 362, 730–732. doi: 10.1038/362730a0

Jewitt, D., and Luu, J. (2004). Crystalline water ice on the Kuiper belt object (50000) Quaoar. *Nature* 432, 731–733. doi: 10.1038/nature03111

Kiss, C., Marton, G., Farkas-Takács, A., Stansberry, J., et al. (2017). Discovery of a satellite of the large trans-neptunian Object (225088) 2007 OR_{10}. *Astrophys. J.* 838:1. doi: 10.3847/2041-8213/aa6484

Kovalenko, I. D., Doressoundiram, A., Lellouch, E., Vilenius, E., Müller, T., and Stansberry, J. (2017). "TNOs are Cool": A survey of the trans-Neptunian region. Astronomy Astrophysics, 608, 19 XIII. Statistical analysis of multiple trans-Neptunian objects observed with Herschel Space Observatory. *Astron. Astrophys.* 608: A19. doi: 10.1051/0004-6361/201730588

Lacerda, P., Fornasier, S., Lellouch, E., Kiss, C., Vilenius, E., Santos-Sanz, P., et al. (2014). The albedo-color diversity of transneptunian objects. *Astrophys. J. Lett.* 793:2. doi: 10.1088/2041-8205/793/1/L2

Lacerda, P., and Jewitt, D. (2007). Densities of solar system objects from their rotational light curves. *Astronom. J.* 133, 1393. doi: 10.1086/511772

Lellouch, E., Moreno, R., Müller, T., Fornasier, S., Santos-Sanz, P., Moullet, A., et al. (2017). The thermal emission of Centaurs and trans-Neptunian objects at millimeter wavelengths from ALMA observations. *Astron. Astrophys.* 608:45. doi: 10.1051/0004-6361/201731676

Lellouch, E., Santos-Sanz, P., Lacerda, P., Mommert, M., Duffard, R., Ortiz, J. L., et al. (2013). "TNOs are Cool": A survey of the trans-Neptunian region. IX. Thermal properties of Kuiper belt objects and Centaurs from combined Herschel and Spitzer observations. *Astron. Astrophys.* 557:60. doi: 10.1051/0004-6361/201322047

Levison, H. F., and Stern, S. A. (2001). On the size dependence of the inclination distribution of the main kuiper belt. *Astronom. J.* 121, 1730–1735. doi: 10.1086/319420

Licandro, J., Ghinassi, F., and Testi, L. (2002). Infrared spectroscopy of the largest known trans-Neptunian object 2001 KX_{75}. *Astron. Astrophys.* 388, L9–L12. doi: 10.1051/0004-6361:20020533

Licandro, J., Oliva, E., and Di Martino, M. (2001). NICS-TNG infrared spectroscopy of trans-neptunian objects 2000 EB173 and 2000 WR106. *Astron. Astrophys.* 373, L29–L32. doi: 10.1051/0004-6361:20010758

Lorenzi, V., Pinilla-Alonso, N., and Licandro, J. (2015). Rotationally resolved spectroscopy of dwarf planet (136472) Makemake. *Astron. Astrophys.* 577:A86. doi: 10.1051/0004-6361/201425575

Lorenzi, V., Pinilla-Alonso, N., Licandro, J., Dalle Ore, C. M., and Emery, J. P. (2014). Rotationally resolved spectroscopy of (20000) Varuna in the near-infrared. *Astron. Astrophys.* 562:A85. doi: 10.1051/0004-6361/201322251

Lykawka, P. S., and Mukai, T. (2005). Higher albedos and size distribution of large transneptunian objects. *P&SS* 53, 1319–1330. doi: 10.1016/j.pss.2005.06.004

Malamud, U., and Prialnik, D. (2015). Modeling Kuiper belt objects Charon, Orcus and Salacia by means of a new equation of state for porous icy bodies. *Icarus* 246, 21–36. doi: 10.1016/j.icarus.2014.02.027

Marsset, M., Fraser, W. C., Pike, R. E., Bannister, M. T., Schwamb, M. E., Volk, K., et al. (2019). Col-OSSOS: Color and Inclination Are Correlated throughout the Kuiper Belt. *arxiv[Preprint]. arXiv:1812.02190.* doi: 10.3847/1538-3881/aaf72e

Mastrapa, R. M. E., and Brown, R. H. (2006). Ion irradiation of crystalline H 2O-ice: effect on the 1. *Icarus* 183, 207–21465-μm band. doi: 10.1016/j.icarus.2006.02.006

McKinnon, W. B., Prialnik, D., Stern, S. A., and Coradini, A. (2008). "Structure and evolution of kuiper belt objects and dwarf planets," in *The Solar System Beyond Neptune,* eds M. A. Barucci, H. Boehnhardt, D. P. Cruikshank, and A. Morbidelli (Tucson: University of Arizona Press), 213–241.

Merk, R., and Prialnik, D. (2006). Combined modeling of thermal evolution and accretion of trans-neptunian objects—Occurrence of high temperatures and liquid water. *Icarus* 183, 283–295. doi: 10.1016/j.icarus.2006.02.011

Merlin, F., Barucci, M. A., de Bergh, C., et al. (2010). Surface composition and physical properties of several trans-neptunian objects from the Hapke scattering theory and Shkuratov model. *Icarus* 208, 945–954. doi: 10.1016/j.icarus.2010.03.014

Merlin, F., Lellouch, E., Quirico, E., and Schmitt, B. (2018). Triton's surface ices: distribution, temperature and mixing state from VLT/SINFONI observations. *Icarus* 314, 274–293. doi: 10.1016/j.icarus.2018.06.003

Milam, S. N., Stansberry, J. A., Sonneborn, G., and Thomas, C. (2016). The James Webb Space Telescope's plan for operations and instrument capabilities for observations in the solar system. *PASP* 959:018001. doi: 10.1088/1538-3873/128/959/018001

Mommert, M., Harris, A. W., Kiss, C., Pál, A., Santos-Sanz, P., Stansberry, J., et al. (2012). TNOs are cool: a survey of the trans-Neptunian region. V. Physical characterization of 18 Plutinos using Herschel-PACS observations. *Astron. Astrophys.* 541:A93. doi: 10.1051/0004-6361/201118562

Morbidelli, A., Levison, H. F., Tsiganis, K., and Gomes, R. (2005). Chaotic capture of Jupiter's Trojan asteroids in the early Solar System. *Nature* 435, 462–465. doi: 10.1038/nature03540

Morbidelli, A., Tsiganis, K., Crida, A., Levison, H. F., and Gomes, R. (2007). Dynamics of the giant planets of the solar system in the gaseous protoplanetary disk and their relationship to the current orbital architecture. *Astronom. J.* 134, 1790–1798. doi: 10.1086/521705

Mueller, T. G., Lellouch , E., Böhnhardt, H., Stansberry, J., Barucci, A., Crovisier, J., et al. (2009). TNOs are Cool: a survey of the transneptunian region. *EMandP* 105, 209–219. doi: 10.1007/s11038-009-9307-x

Nesvorny, D. (2015a). Jumping neptune can explain the kuiper belt kernel. *Astronom. J.* 150:68. doi: 10.1088/0004-6256/150/3/68

Nesvorny, D. (2015b). Evidence for slow migration of neptune from the inclination distribution of kuiper belt objects. *Astronom. J.* 150:73. doi: 10.1088/0004-6256/150/3/73

Nesvorny, D., and Morbidelli, A. (2012). Statistical study of the early solar system's instability with four, five, and six giant planets. *Astronom. J.* 144:117. doi: 10.1088/0004-6256/144/4/117

Nesvorny, D., and Vokrouhlicky, D. (2016). Neptune's orbital migration was grainy, not smooth. *Astrophys. J.* 825:94. doi: 10.3847/0004-637X/825/2/94

Noll, K. S., Grundy, W. M., Chiang, E. I., Margot, J.-L., and Kern, S. D. (2008a). "Binaries in the Kuiper Belt," in *The Solar System Beyond Neptune,* eds M. A. Barucci, H. Boehnhardt, D. P. Cruikshank, and A. Morbidelli (Tucson: University of Arizona Press), 592, 345–363.

Noll, K. S., Grundy, W. M., Stephens, D. C., Levison, H. F., and Kern, S. D. (2008b). Evidence for two populations of classical transneptunian objects: the strong inclination dependence of classical binaries. *Icarus* 194, 758–768. doi: 10.1016/j.icarus.2007.10.022

Noll, K. S., Levison, H. F., Grundy, W. M., and Stephens, D. C. (2006). Discovery of a binary Centaur. *Icarus* 184, 611–618. doi: 10.1016/j.icarus.2006.05.010

Pál, A., Kiss, C., Müller, T. G., Molnár, L., Szab,ó, R., et al. (2016). Large size and slow rotation of the trans-Neptunian Object (225088) 2007 OR_{10} Discovered from Herschel and K2 Observations. *Astronom. J.* 151:117. doi: 10.3847/0004-6256/151/5/117

Parker, A., Pinilla-Alonso, N., Santos-Sanz, P., Stansberry, J., Alvarez-Candal, A., Bannister, M., et al. (2016). Physical characterization of TNOs with the James Webb Space Telescope. *PASP* 128:018010. doi: 10.1088/1538-3873/128/959/018010

Parker, A. H., Kavelaars, J. J., Petit, J.-M., Jones, L., Gladman, B., and Parker, J. (2011). Characterization of seven ultra-wide trans-neptunian binaries. *Astrophys. J.* 743:1. doi: 10.1088/0004-637X/743/1/1

Peixinho, N., Boehnhardt, H., Belskaya, I., Doressoundiram, A., Barucci, M. A., and Delsanti, A. (2004). ESO large program on Centaurs and TNOs: visible colors—final results. *Icarus* 170, 153–166. doi: 10.1016/j.icarus.2004.03.004

Peixinho, N., Delsanti, A., and Doressoundiram, A. (2015). Reanalyzing the visible colors of Centaurs and KBOs: what is there and what we might be missing. *Astron. Astrophys.* 577:A35. doi: 10.1051/0004-6361/201425436

Peixinho, N., Delsanti, A., Guilbert-Lepoutre, A., Gafeira, R., and Lacerda, P. (2012). The bimodal colors of Centaurs and small Kuiper belt objects. *Astron. Astrophys.* 546:A86. doi: 10.1051/0004-6361/201219057

Peixinho, N., Doressoundiram, A., Delsanti, A., Boehnhardt, H., Barucci, M. A., and Belskaya, I. (2003). Reopening the TNOs color controversy: Centaurs bimodality and TNOs unimodality. *Astron. Astrophys.* 410, 29–32. doi: 10.1051/0004-6361:20031420

Peixinho, N., Lacerda, P., and Jewitt, D. (2008). Color-inclination relation of the classical kuiper belt objects. *Astronom. J.* 136, 1837–1845. doi: 10.1088/0004-6256/136/5/1837

Perna, D., Dotto, E., Barucci, M. A., Mazzotta Epifani, E., Vilenius, E., Dall'Ore, M., et al. (2013). Photometry and taxonomy of trans-Neptunian objects and Centaurs in support of a Herschel key program. *Astron. Astrophys.* 554:A49. doi: 10.1051/0004-6361/201219859

Perna, D., Hromakina, T., Merlin, F., Ieva, S., Fornasier, S., Belskaya, I., et al. (2017). The very homogeneous surface of the dwarf planet Makemake. *Monthly Notices of the RAS* 466, 3594–3599. doi: 10.1093/mnras/stw3272

Pike, R. E., Fraser, W. C., Schwamb, M. E., Kavelaars, J. J., Marsset, M., Bannister, M. T., et al. (2017). Col-OSSOS: z-band photometry reveals three distinct TNO surface types. *Astronom. J.* 154:101. doi: 10.3847/1538-3881/aa83b1

Poston, M. J., Mahjoub, A., Ehlmann, B. L., Blacksberg, J., Brown, M. E., Carlson, R. W., et al. (2018). Visible near-infrared spectral evolution of irradiated mixed ices and application to kuiper belt objects and jupiter trojans. *Astrophys. J.* 856:124. doi: 10.3847/1538-4357/aab1f1

Santos-Sanz, P., Lellouch, E., Fornasier, S., Kiss, C., Pal, A., Müller, T. G., et al. (2012). "TNOs are Cool": a survey of the trans-Neptunian region. IV. Size/albedo characterization of 15 scattered disk and detached objects observed with Herschel-PACS. *Astron. Astrophys.* 541:A92. doi: 10.1051/0004-6361/201118541

Schaller, E. L., and Brown, M. E. (2007a). Volatile loss and retention on kuiper belt objects. *Astrophys. J. Lett.* 659, 61–64. doi: 10.1086/516709

Schaller, E. L., and Brown, M. E. (2007b). Detection of methane on kuiper belt object (50000) Quaoar. *Astrophys. J. Lett.* 670, 49–51. doi: 10.1086/524140

Schaller, E. L., and Brown, M. E. (2008). Detection of additional members of the 2003 EL61 collisional family via near-infrared spectroscopy. *Astrophys. J.* 684:L107. doi: 10.1086/592232

Schmitt, B., Bollard, P., Albert, D., Garenne, A., Bonal, L., and the SSHADE partner's consortium (2018). SSHADE: "Solid Spectroscopy Hosting Architecture of Databases and Expertise" and its databases. OSUG Data Center. Service/Database Infrastructure. doi: 10.17178/SSHADE

Shchuko, O. B., Shchuko, S. D., Kartashov, D. V., and Orosei, R. (2014). Conditions for liquid or icy core existence in KBO objects: Numerical simulations for Orcus and Quaoar. *PSS* 104, 147–155. doi: 10.1016/j.pss.2014.01.022

Souza-Feliciano, A. C., Alvarez-Candal, A., and Jiménez-Teja, Y. (2018). Wavelet theory applied to the study of spectra of trans-Neptunian objects. *Astron. Astrophys.* 614:A92. doi: 10.1051/0004-6361/201731464

Stansberry, J., Grundy, W., Brown, M., Cruikshank, D., Spencer, J., Trilling, D., et al. (2008). "Physical properties of kuiper belt and centaur objects: constraints from the spitzer space telescope," in *The Solar System Beyond Neptune,* eds M. A. Barucci, H. Boehnhardt, D. P. Cruikshank, and A. Morbidelli (Tucson:University of Arizona Press), 592, 161–179.

Stansberry, J. A., Grundy, W. M., Mueller, M., Benecchi, S. D., Rieke, G. H., Noll, K. S., et al. (2012). Physical properties of trans-neptunian binaries (120347) Salacia-Actaea and (42355) Typhon-Echidna. *Icarus* 219, 676–688. doi: 10.1016/j.icarus.2012.03.029

Strazzulla, G., and Palumbo, M. E. (1998). Evolution of icy surfaces: an experimental approach. *PandSS* 46, 1339–1348. doi: 10.1016/S0032-0633(97)00210-9

Tancredi, G. (2010). Physical and dynamical characteristics of icy "dwarf planets" (plutoids). *IAUS* 263:173. doi: 10.1017/S1743921310001717

Tegler, S. C., and Romanishin, W. (1998). Two distinct populations of Kuiper-belt objects. *Nature* 392, 49–51. doi: 10.1038/32108

Tegler, S. C., and Romanishin, W. (2000). Extremely red Kuiper-belt objects in near-circular orbits beyond 40 AU. *Nature* 407, 979–981. doi: 10.1038/35039572

Tegler, S. C., Romanishin, W., and Consolmagno, G. J. (2003). Resolution of the kuiper belt object color controversy: two distinct color populations. *Astrophys. J.* 599, 49–52. doi: 10.1086/381076

Tegler, S. C., Romanishin, W., and Consolmagno, G. J. (2016). Two color populations of kuiper belt and centaur objects and the smaller orbital inclinations of red centaur objects. *Astronom. J.* 152:210. doi: 10.3847/0004-6256/152/6/210

Thirouin, A., Noll, K. S., Ortiz, J. L., and Morales, N. (2014). Rotational properties of the binary and non-binary populations in the trans-Neptunian belt. *Astron. Astrophys.* 569:A3. doi: 10.1051/0004-6361/201423567

Trujillo, C. A., and Brown, M. E. (2002). A Correlation between Inclination and Color in the Classical Kuiper Belt. *Astrophys. J.* 566, 125–128. doi: 10.1086/339437

Trujillo, C. A., Brown, M. E., Rabinowitz, D. L., and Geballe, T. R. ,(2005). Near-infrared surface properties of the two intrinsically brightest minor planets: (90377) Sedna and (90482) Orcus. *Astrophys. J.* 627:1057. doi: 10.1086/430337

Trujillo, C. A., Sheppard, S. S., and Schaller, E. L. (2011). A photometric system for detection of water and methane ices on kuiper belt objects. *Astrophys. J.* 730:105. doi: 10.1088/0004-637X/730/2/105

Tsiganis, K., Gomes, R., Morbidelli, A., and Levison, H. F. (2005). Origin of the orbital architecture of the giant planets of the Solar System. *Nature* 435, 459–461. doi: 10.1038/nature03539

Vachier, F., Berthier, J., and Marchis, F. (2012). Determination of binary asteroid orbits with a genetic-based algorithm. *Astron. Astrophys.* 543:A68. doi: 10.1051/0004-6361/201118408

Vilenius, E., Kiss, C., Mommert, M., Müller, T., Santos-Sanz, P., Pal, A., et al. (2012). "TNOs are Cool": A survey of the trans-Neptunian region. VI. Herschel/PACS observations and thermal modeling of 19 classical Kuiper belt objects. *Astron. Astrophys.* 541:A94. doi: 10.1051/0004-6361/201118743

Vilenius, E., Kiss, C., Müller, T., Mommert, M., Santos-Sanz, P., Pál, A., et al. (2014). "TNOs are Cool": a survey of the trans-Neptunian region. Analysis of classical Kuiper belt objects from Herschel and Spitzer observations. *Astron. Astrophys.* 564, A35. doi: 10.1051/0004-6361/201322416

Walsh, K. J., Morbidelli, A., Raymond, S. N., O'Brien, D. P., and Mandell, A. M. (2011). A low mass for Mars from Jupiter's early gas-driven migration. *Nature* 475, 206–209. doi: 10.1038/nature10201

Wong, I., and Brown, M. E. (2017). The bimodal color distribution of small kuiper belt objects. *Astronom. J.* 153:145. doi: 10.3847/1538-3881/aa60c3

Conflict of Interest Statement: The authors declare that the research was conducted in the absence of any commercial or financial relationships that could be construed as a potential conflict of interest.